Pure Appl. Chem., Vol. 84, No. 4, pp. 1089–1100, 2012.
http://dx.doi.org/10.1351/PAC-CON-11-09-09

Bowl-to-bowl inversion of sumanene derivatives*

Toru Amaya and Toshikazu Hirao‡

Department of Applied Chemistry, Graduate School of Engineering, Osaka University, Yamada-oka, Suita, Osaka 565-0871, Japan

Abstract: Bowl-to-bowl inversion is one of the characteristic behaviors for some flexible open-end molecular bowls consisting of polycyclic aromatic hydrocarbons with benzene rings fused by imbedded five-membered rings (π bowls). This intriguing dynamics was studied with sumanene, which is the smallest C_{3v} symmetric fragment of fullerenes. In this article, our ongoing research on the bowl-to-bowl inversion of sumanene, its benzylic anion species, hexasubstituted derivatives, mononaphthosumanene, and [CpRu(η^6-sumenene)]$^+$ complex is summarized. Estimation based on density functional theory (DFT) calculation is also described.

Keywords: bowl-to-bowl inversion; π bowl; π bowl complex; density functional theory (DFT); polycyclic aromatic hydrocarbons; sumanene.

INTRODUCTION

Open-end molecular bowls consisting of polycyclic aromatic hydrocarbons with benzene rings fused by imbedded five-membered rings attract interest in the science of nonplanar π-conjugated carbon systems in addition to fullerenes and carbon nanotubes (the term "π bowl" is used for such compounds in the present article, whereas they have been also called open geodesic polyarene [1] or buckybowl [2]) [3–9]. Bowl-to-bowl inversion is one of the characteristic behaviors for some flexible π bowls (Fig. 1a). This intriguing dynamics has been exclusively studied with corannulene (**2a**, Fig. 1b), which is the smallest C_{5v} symmetric fragment of fullerenes with the bowl depth of 0.87 Å [10], and its derivatives. Scott and co-workers demonstrated for the first time that the bowl-to-bowl inversion of the corannulene derivative **2b** occurs rapidly with the activation barrier of 10–11 kcal mol^{-1} [11]. Further elaboration of the structures gave more detailed insight into the inversion dynamics, for example, the introduction of the rigid five-membered ring to the rim of corannulene was found to slow the inversion by Sygula and Rabideau et al. [12,13]. Siegel and co-workers investigated the relationship between the inversion energy barrier and the bowl depth [14]. In this regard, sumanene (**1**, Fig. 1b) with the deeper C_{3v} symmetric bowl (1.11 Å) is another candidate molecule to investigate the inversion behavior [15,16]. Furthermore, the facile functionalization using three benzylic positions permits the structural elucidation [16–19]. In this article, we summarize our ongoing research on bowl-to-bowl inversion of sumanene derivatives and complex. The behavior is also estimated by density functional theory (DFT) calculation.

Pure Appl. Chem.* **84, 861–1112 (2012). A collection of invited papers based on presentations at the 14th International Symposium on Novel Aromatic Compounds (ISNA-14), Eugene, OR, USA, 24–29 July 2011.

‡Corresponding author

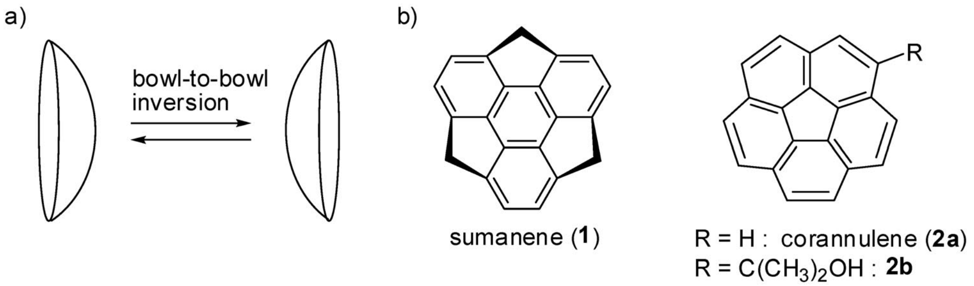

Fig. 1 (a) Schematic representation of bowl-to-bowl inversion of π bowl. (b) Sumanene (**1**) and corannulenes **2a** and **2b**.

BOWL-TO-BOWL INVERSION OF SUMANENE

In the ^{1}H NMR spectrum of sumanene (**1**), a characteristic pair of doublets at 3.42 and 4.71 ppm was observed, assignable to the *endo*- and *exo*-benzylic protons, respectively [15]. Variable-temperature NMR of sumanene in *p*-xylene-d_{10} solution revealed that the inversion barrier $\Delta G^{\ddagger}$ is estimated as more than 19.4 kcal mol^{-1}.

More detailed investigation was carried out by 2D exchange spectroscopy (EXSY) NMR experiments. Trideuteriosumanene **3** was used to measure the bowl-to-bowl inversion (Fig. 2). In this molecule, the bowl-to-bowl inversion is equivalent to the isomerization between the diastereomers. Accordingly, estimation of the isomerization rate quantified by the cross-peaks in a 2D-EXSY NMR spectrum gives the inversion rate. From such experiments in CDCl$_3$, the activation energy of 20.4 kcal mol^{-1} at 318 K was obtained (Table 1, entry 1) [20], which is approximately twice as high as for the corannulene derivative **2b**. The use of CD$_2$Cl$_2$ and THF-d_8 showed similar values (Table 1, entries 2 and 3). On the other hand, the use of methylated benzene-based solvents (toluene-d_8, *p*-xylene-d_{10}, and mesitylene-d_{12}) exhibited the tendency of decreasing the energy barrier (Table 1, entries 6–8, 19.7–19.9 kcal mol^{-1}). The difference between the highest and the lowest value reached 0.7 kcal mol^{-1}, therefore, the inversion of **3** can be accelerated up to three times by simply exchanging the solvent (0.066 s^{-1} for CDCl$_3$ and 0.21 s^{-1} for *p*-xylene-d_{10} at 318 K).

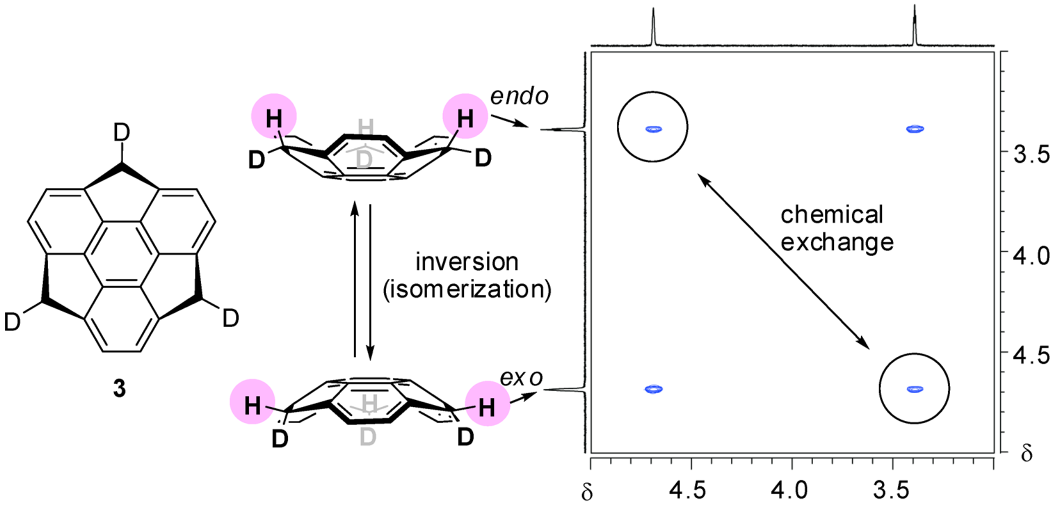

Fig. 2 Trideuteriosumanene **3**, a schematic representation of its bowl-to-bowl inversion, and a selected region of the 2D-EXSY NMR spectrum of **3** in CDCl$_3$ at 318 K.

Table 1 Rate constant k (s^{-1}) and activation energy $\Delta G^{\ddagger}$ (kcal mol^{-1}) for the bowl-to-bowl inversion (600 MHz, 318 K, 20 mM).[a]

Entry	Solvent	k (s^{-1})	$\Delta G^{\ddagger}$ (kcal mol^{-1})[b]
1	$CDCl_3$	0.066	20.4
2	CD_2Cl_2	0.015 (303 K)	20.3 (303 K)
3	THF-d_8	0.075	20.3
4	1,4-Dioxane-d_8	0.10	20.1
5	Benezene- d_6	0.089	20.2
6	Toluene-d_8	0.13	19.9
7	*p*-Xylene-d_{10}	0.21	19.7
8	Mesitylene-d_{12}	0.15	19.9

[a] All experiments were carried out twice, and the errors did not exceed 0.1 %. All 2D-EXSY NMR spectra were clear enough to quantify the area of the cross-peaks.

[b] $\Delta G^{\ddagger} = -RT\ln(hk/k_BT)$: T is temperature, k_B is the Boltzmann constant, and h is the Planck constant.

BOWL-TO-BOWL INVERSION OF SUMANENE'S BENZYLIC ANION SPECIES

As mentioned in the introduction, sumanene (**1**) is characterized by its benzylic positions, where the corresponding radicals, cations, anions, carbenes, etc. are stabilized. In fact, the mono-, di-, and trianions are stepwise generated by treatment with the requisite amount of *t*-BuLi [16].

The dynamic behaviors of the monoanion **4** and dianion **5** were investigated. Treatment of **3** with the requisite amount of *t*-BuLi generated **4** and **5**. The inversion behavior was first studied using 2D-EXSY NMR experiments in THF-d_8. However, no cross-peak was observed in both of them. It suggests that the anions **4** and **5** maintain a relatively rigid bowl shape [20]. So, we planned to monitor the equilibration of *exo*-deuterated **4a** and **5a** by simple ^1H NMR measurement to investigate such slow inversion. Selective deuteration of the trianion was achieved to give **3a** by precipitation with CH_3OD at approximately –100 °C (Fig. 3a). Keeping **3a** as a solid at room temperature did not induce the bowl-to-bowl inversion. To generate monoanion **4a** and dianion **5a**, **3a** was treated with the requisite amount of *t*-BuLi at approximately –100 °C in THF-d_8 (Figs. 3b,c), then the equilibration was monitored, respectively. The ^1H NMR spectra are shown in Figs. 3b,c. Growing of the *exo*-protons (4.46 and 3.88 ppm for **4** and **5**, respectively) was observed in both spectra (Figs. 3b,c) [20]. The half-life times were 2755 s for **4** at 283 K and 7580 s for **5** at 273 K. The rate constants (*k*s) for the reversible equilibration of **4** and **5** were $9.10 \times 10^{-5}\ s^{-1}$ at 283 K and $3.40 \times 10^{-5}\ s^{-1}$ at 273 K, respectively, determined by regression analysis using the equation $2kt = \ln[a/(a-2x)]$ where a is the initial concentration of **4a** (or **5a**) and x is the concentration of **4b** (or **5b**) at time t. Correlation coefficients of the linear regressions were 0.999 and 0.978. $\Delta G^{\ddagger}$s were 21.8 and 21.5 kcal mol^{-1} for **4** and **5**, respectively, calculated from the Eyring equation. Monoanion **4** and dianion **5** possess 1.5 and 1.2 kcal mol^{-1} higher barrier than that of **3**, respectively.

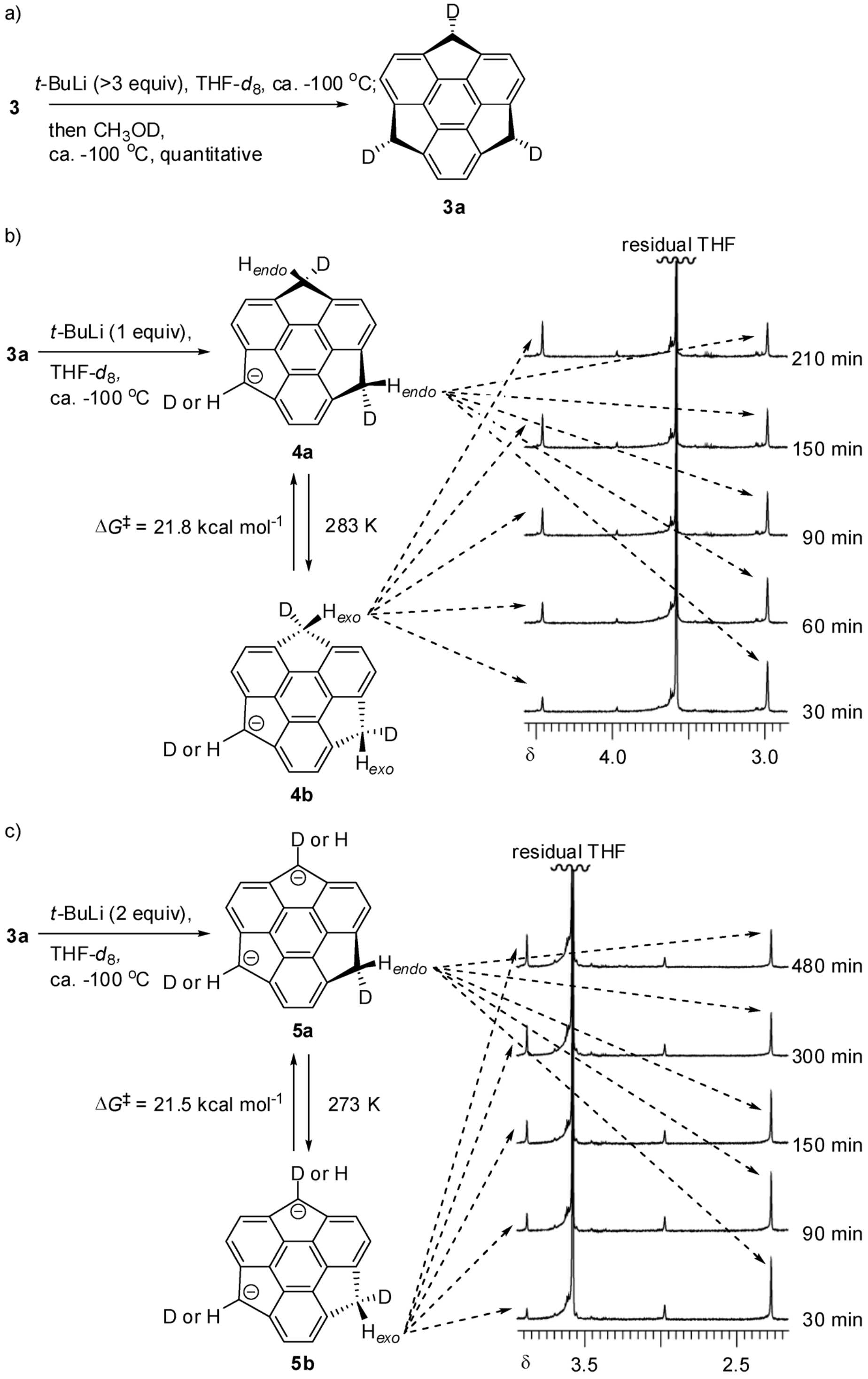

Fig. 3 (a) Synthesis of *exo*-trideuterated sumanene **3a**. (b) Generation of monoanion **4a** and selected ^{1}H NMR spectra for the equilibration at 283 K (600 MHz, 22 mM, THF-d_8). (c) Generation of dianion **5a** and selected ^{1}H NMR spectra for the equilibration at 273 K (600 MHz, 22 mM, THF-d_8).

LOCKING OF BOWL-TO-BOWL INVERSION IN *EXO*-SUBSTITUTED TRIS(TRIMETHYLSYLYL)SUMANENE

The reaction of the benzylic trianion with an electrophile was demonstrated by quantitative trapping with chlorotrimethylsilane, in which the *exo*-introduced tris(trimethylsilyl) derivative **6** was obtained with perfect selectivity, probably due to the steric demand (Scheme 1) [16]. Interestingly, bowl-to-bowl inversion of **6** was not observed in the variable-temperature NMR study. The tri-introduction of the trimethylsilyl group in the benzylic *exo*-position looks to lock the bowl-to-bowl inversion (or the equilibrium of the inversion might dominantly tilt to this isomer side).

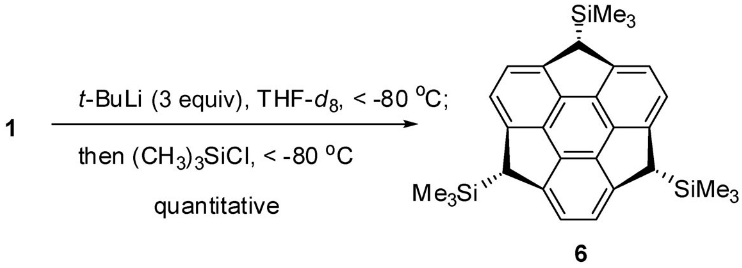

Scheme 1 Synthesis of tris(trimethylsilyl)sumanene **6**.

BOWL-TO-BOWL INVERSION OF HEXASUBSTITUTED SUMANENES

The hexaallylated and hexa-*p*-methoxybenzylated sumanenes **7** and **8** were obtained by nucleophilic substitution reaction of **1** with aqueous 30 % NaOH solution as a base in the presence of a catalytic amount of tetrabutylammonium bromide and a minimum amount of THF in quantitative and 75 % yields, respectively (Scheme 2) [20]. Full characterization for all protons and carbons was carried out by ^{1}H NMR, ^{13}C NMR, 2D nuclear Overhauser spectroscopy (NOESY), heteronuclear multiple-bond correlation (HMBC), and heteronuclear multiple-quantum coherence (HMQC) experiments. The chemical exchange of H_a-$H_{a'}$ and H_b-$H_{b'}$ was analyzed for **7** and **8**, respectively. The inversion barriers of **7** and **8** were 19.2 and 18.2 kcal mol^{-1} at 318 K, which are 1.2 and 2.2 kcal mol^{-1} lower than that of **3**, respectively [20]. In terms of the inversion rate, these values are approximately 7 and 35 times as fast as that of **3**. The facile inversion of hexasubstituted sumanenes may be due to the steric repulsion of the bulky *endo*-substituents.

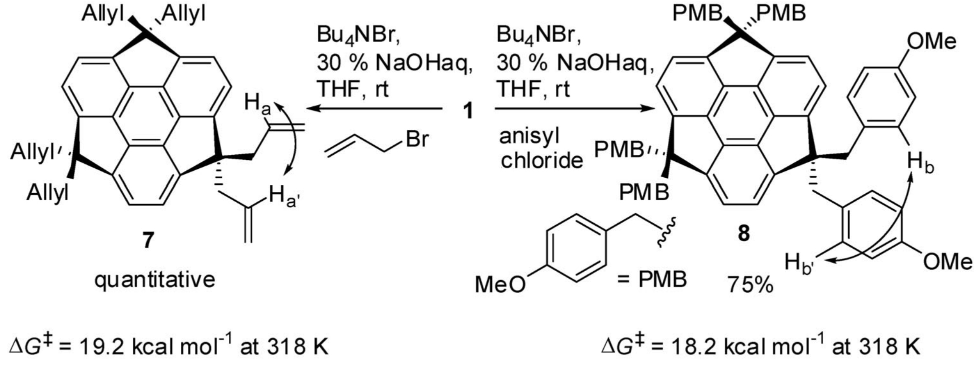

Scheme 2 Synthesis of the hexaallylated and hexa-*p*-methoxybenzylated sumanenes **7** and **8**.

BOWL-TO-BOWL INVERSION OF MONONAPHTHOSUMANENE

An additional fused ring on the sumanene structure is considered to slow the bowl inversion. In the study of the inversion dynamics for corannulenes, the additional five-membered ring effectively slows the inversion (ca. 27.65 kcal mol^{-1}) [12,13].

Mononaphthosumanene **9** was synthesized via intramolecular dehydrative benzannulation of monoaldehyde, which was prepared through Suzuki–Miyaura coupling reaction of bromosumanene [21] with 2-formylphenylboronic acid [18]. Bowl-to-bowl inversion was examined by the conversion to dideuterated **9a**, where the inversion is equivalent to the isomerization between the diastereomers **9a** and **9b** (Fig. 4). As the inversion was not observed at room temperature, the equilibration between **9a** and **9b** was monitored in mesitylene-d_{12} at 140 °C by ^{1}H NMR. Growing of the peaks for *exo*-protons (δ 4.42 and 4.54) was observed over a period of hours, as shown in Fig. 4. The observed rate constant (k) and inversion barrier ($\Delta G^{\ddagger}$) of **9a** are 8.20×10^{-5} s^{-1} and 32.2 kcal mol^{-1} [18], which is almost 10 kcal mol^{-1} higher than that of **3**.

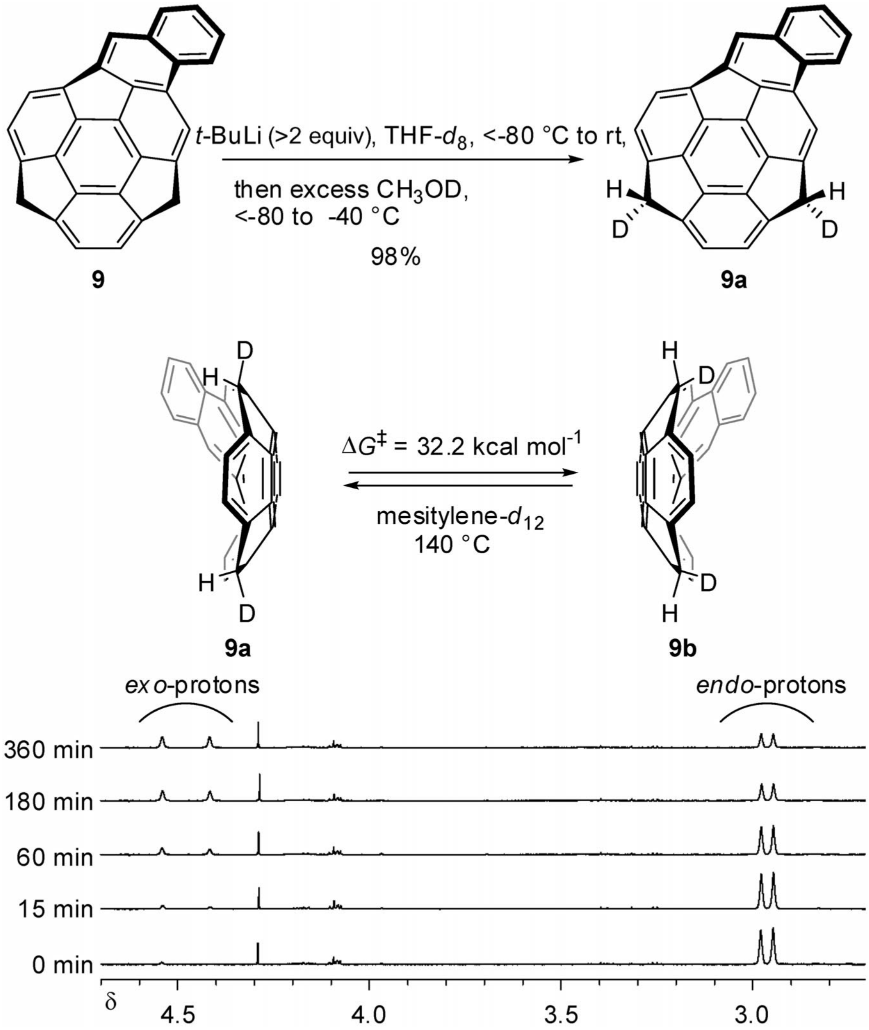

Fig. 4 Synthesis of *exo*-dideuterated mononaphthosumanene **9a**, its bowl-to-bowl inversion, and the selected ^{1}H NMR spectra for the equilibration at 413 K (600 MHz, mesitylene-d_{12}).

BOWL-TO-BOWL INVERSION OF [CpRu(SUMANENE)]$^+$ COMPLEX

From a coordination chemistry viewpoint, π bowls are unique ligands because they can provide not only convex surfaces but also open concave surfaces for metal binding. π-Bowl complexes of various metals in several coordination modes have been prepared and characterized for over a decade [8,22,23]. We have also studied the complexation of sumanene, and demonstrated the first concave-selective binding complex [CpFe(η^6-sumanene)]PF_6 ($Cp=C_5H_5$) [24–26]. However, the bowl-to-bowl inversion has not been elucidated with π-bowl transition-metal complexes until our study for [CpRu(sumanene)]$^+$ complex **10** (Fig. 5a).

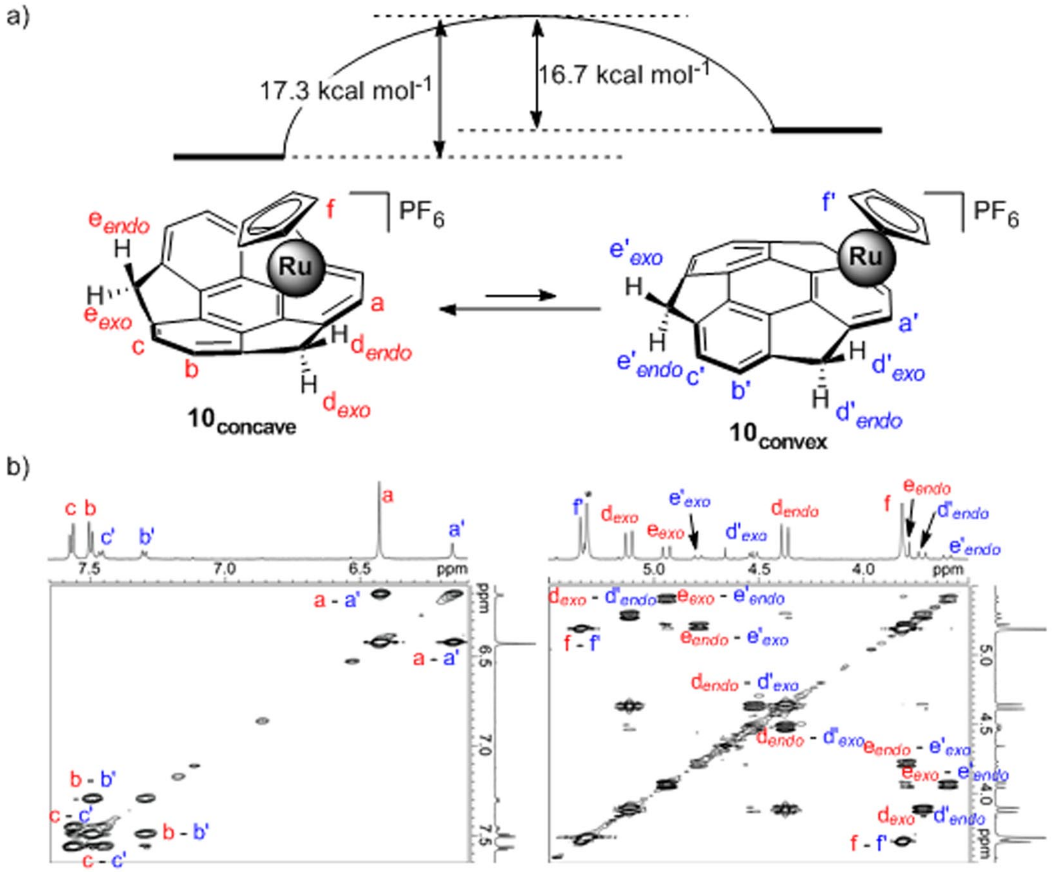

Fig. 5 (a) Bowl-to-bowl inversion of [CpRu(sumanene)]PF_6 (**10**). (b) 2D-EXSY NMR spectra of **10** in CD_2Cl_2.

The complex **10** was synthesized by ligand exchange with a Cp group of ruthenocene in the presence of sumanene, aluminum powder, and aluminum chloride without solvent under argon at 135 °C [27]. A pair of two species was observed in the ^{1}H NMR spectra of [CpRu(sumanene)]PF_6 (**10**). The major and minor species were assigned to the concave-bound complex $\mathbf{10}_{\mathbf{concave}}$ and the convex-bound isomer $\mathbf{10}_{\mathbf{convex}}$, respectively, by NOE experiments. The ratio of the concave and convex complexes depends to some degree on the solvent. In CD_2Cl_2, the ratio in the equilibrium is 75/25 for $\mathbf{10}_{\mathbf{concave}}/\mathbf{10}_{\mathbf{convex}}$ at 298 K. In more polar solvents, the equilibrium tends to the major isomer $\mathbf{10}_{\mathbf{concave}}$ (up to 90 % in CD_3CN and CD_3NO_2). 2D-EXSY NMR experiment of **10** clearly showed negative cross-peaks for the chemical exchange between H_{a-f} and $H_{a'-f'}$ in one-to-one correspondence, as exemplified by a–a' (Fig. 5b). The *endo*-benzylic protons $H_{d\mathit{endo}}$ and $H_{e\mathit{endo}}$ of $\mathbf{10}_{\mathbf{concave}}$ show correlations with the *exo*-benzylic peaks $H_{d'\mathit{exo}}$ and $H_{e'\mathit{exo}}$ of $\mathbf{10}_{\mathbf{convex}}$ (at 4.53 and 4.79 ppm, respectively), which are in a common region for *exo*-benzylic protons. Conversely, the *exo*-benzylic protons $H_{d\mathit{exo}}$ and $H_{e\mathit{exo}}$ of $\mathbf{10}_{\mathbf{concave}}$ showed correlations with the *endo*-benzylic peaks $H_{d'\mathit{endo}}$ and $H_{e'\mathit{endo}}$ of $\mathbf{10}_{\mathbf{convex}}$ (at 3.72 and 3.60 ppm, respectively), which are in a typical region for *endo*-benzylic protons. The bowl-to-bowl inversion can account for the phenomenon without inconsistency. The quantification of the cross-peaks in CD_2Cl_2 gives an inversion barrier of 16.7 and 17.3 kcal mol^{-1} at 303 K for $\mathbf{10}_{\mathbf{convex}}$ to $\mathbf{10}_{\mathbf{concave}}$ and the reverse inversion, respectively (Fig. 5a) [27]. Linear van't Hoff plots give a positive ΔH and a negative ΔS.

From a mixture of the diastereomers, a single crystal of $\mathbf{10}_{\mathbf{concave}}$, which is the major species, was obtained. In the X-ray crystallographic analysis, ORTEP diagrams clearly showed the concave-coordination (Fig. 6) [27]. Once the crystal of $\mathbf{10}_{\mathbf{concave}}$ was dissolved, both isomers of **10** appeared again. These results indicate that the preference of the concave or convex isomer is considered to be under thermodynamic control.

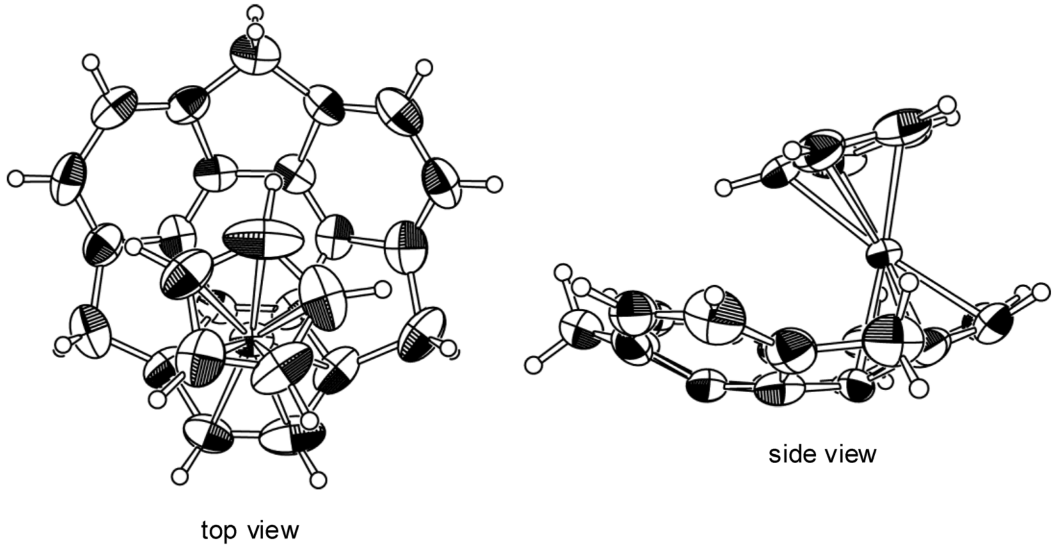

Fig. 6 ORTEP drawings of $\mathbf{10}_{\mathbf{concave}}$ in top and side views. The hexafluorophosphate anion is omitted for clarity.

BOWL-TO-BOWL INVERSION STUDY USING CIRCULAR DICHROMISM (CD)

As described above, NMR methods are a powerful tool for investigating the bowl-to-bowl inversion dynamics. As another method, circular dichromism (CD) experiments can be used by following the racemization of an enantiopure π bowl in case the bowl-to-bowl inversion corresponds to the racemization. This method is complementary for the NMR methods. Sakurai and co-workers showed the efficiency of this method for the inversion of trimethylsumanene **11** and trimethylsumanenetrione **12** (21.6 kcal mol^{-1} in CH_3CN at 233 K for **11** [28], 23.4 kcal mol^{-1} in CH_3CN at 300 K for **12** [29]) (Fig. 7).

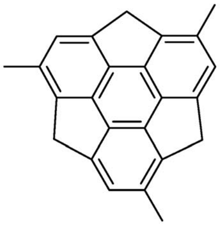

11

$\Delta G^{\ddagger}$ = 21.6 kcal mol^{-1} in CH_3CN at 233 K

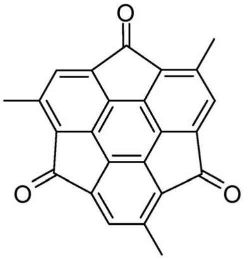

12

$\Delta G^{\ddagger}$ = 23.4 kcal mol^{-1} in CH_3CN at 300 K

Fig. 7 Trimethylsumanene **11** and trimethylsumanenetrione **12**.

ESTIMATION OF ACTIVATION ENERGY FOR BOWL-TO-BOWL INVERSION OF SUMANENES BASED ON DFT CALCULATION

Estimation of bowl-to-bowl inversion based on calculation has been investigated since the report of the dynamics of a corannulene derivative. Correlation between a bowl depth x and an energy barrier E_a ($E_a = Cx^4$) is suggested [14]. Bowl-to-bowl inversion of sumanene (**1**) also has been studied. Theoretical calculation using DFT method suggested that the inversion barrier of **1** is 16.9 kcal mol^{-1} (B3LYP/cc-pVTZ//B3LYP/cc-pVDZ, Gaussian 94) [30].

With some experimental values in hand, the bowl-to-bowl inversion of **1**, its benzylic monoanion **13** ($C_{21}H_{11}^{-}$), dianion **14** ($C_{21}H_{10}^{2-}$), and trianion **15** ($C_{21}H_{9}^{3-}$), and naphthosumanenes **9**, **16a**, **16b**, and **17** were theoretically studied.

Bowl-to-bowl inversion barriers were estimated from the energy difference between the optimized bowl structure and the planar structure for a transition state, as reported previously [30]. All calculations were conducted using a Gaussian 03 suite program. All the bowl-shaped compounds were structurally optimized at the B3LYP/6-31G(d,p) level. Planar conformers for the transition states were optimized at the same level of theory, and the structures were checked using the corresponding frequency calculation. Single-point energy calculation was conducted for these optimized structures to evaluate the bowl-to-bowl inversion barriers. After trial of some calculated conditions, use of B3LYP/6-311^{+}G(2d,p) approximately reproduced the experimental values. Therefore, these conditions were employed for the sumanene derivatives. Table 2 summarizes both experimental and calculated values [31]. The calculation mainly reproduced the experimental values well, whereas calculation tends to slightly underestimate the barrier. The inversion barrier for trinaphthosumanene **17** was calculated to be 63.8 kcal mol^{-1} (Table 2, entry 8). Apparently, its bowl structure is difficult to invert.

Table 2 Bowl-to-bowl inversion barriers $\Delta G^{\ddagger}$ (kcal mol^{-1}) for **1**, **9**, **13**, **14**, **15**, **16a**, **16b**, and **17**.

Entry	Compound	$\Delta G^{\ddagger}$ (kcal mol^{-1})	
		Experimental	Calculated[a]
1	Sumanene (**1**)	19.7–20.4[b]	19.0
2	Monoanion **13**	21.8[c]	21.6
3	Dianion **14**	21.5[d]	22.5
4	Trianion **15**	–	20.9
5	Mononaphthosumanene **9**	32.2[e]	31.4
6	Dinaphthosumanene **16a**	–	46.4
7	Dinaphthosumanene **16b**	–	45.2
8	Trinaphthosumanene **17**	–	63.8

[a] B3LYP/6-311^{+}G(2d,p)//B3LYP/6-31G(d,p).
[b] Obtained from **3**.
[c] Obtained from **4a**.
[d] Obtained from **5a**.
[e] Obtained from **9a**.

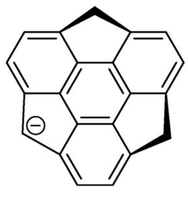
13

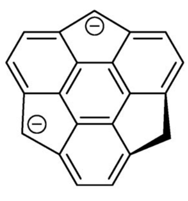
14

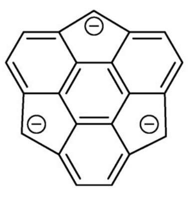
15

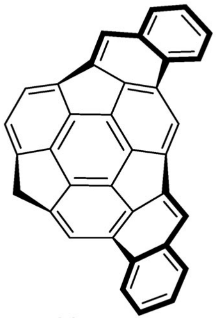
16a

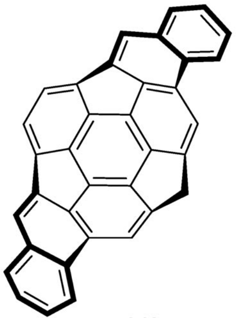
16b

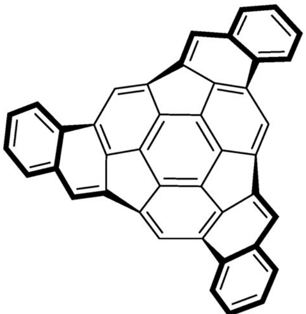
17

SUMMARY

In summary, the bowl-to-bowl inversion of sumanene derivatives was focused on, and discussed based on the inversion barrier. $\Delta G^{\ddagger}$ of the deuteriosumanene **3** was 19.7–20.4 kcal mol^{-1}, depending on the solvents. The mono- and dianions of **3** showed the relatively rigid structure in solution (21.8 and 21.5 kcal mol^{-1}, respectively). Hexasubstituted derivatives **7** and **8** exhibited the low inversion barriers (19.2 and 18.2 kcal mol^{-1}, respectively). On the other hand, substitution with the trimethylsilyl group in the benzylic *exo*-positions looks to lock the inversion. Mononaphthosumanene **9** showed the barrier 32.2 kcal mol^{-1}. The bowl-to-bowl inversion behavior in the solution of a π-bowl complex [CpRu(sumanene)]PF$_6$ (**10**) was investigated by 2D-EXSY NMR. To estimate the activation energy of sumanene derivatives based on DFT calculation, use of B3LYP/6-311^{+}G(2d,p) is beneficial. The obtained dynamic aspect on bowl-to-bowl inversion is envisioned to lead a molecular switch or a molecular machine based on sumanene.

ACKNOWLEDGMENTS

We thank all of our talented co-workers for their great contributions reported in this account. This work was partially supported by Grants-in-Aid for Scientific Research (A) (22245007), Young Scientists (A) (22685006), and Challenging Exploratory Research (23655048) from the Japan Society for the Promotion of Science. Financial support from the Japan Science and Technology Agency (A-STEP, No AS2211281D) is also acknowledged.

REFERENCES

1. L. T. Scott, H. E. Bronstein, D. V. Preda, R. B. M. Ansems, M. S. Bratcher, S. Hagen. *Pure Appl. Chem.* **71**, 209 (1999).
2. P. W. Rabideau, A. H. Abdourazak, H. E. Folsom, Z. Marcinow, A. Sygula, R. Sygula. *J. Am. Chem. Soc.* **116**, 7891 (1994).
3. P. W. Rabideau, A. Sygula. *Acc. Chem. Res.* **29**, 235 (1996).
4. G. Mehta, H. S. P. Rao. *Tetrahedron* **54**, 13325 (1998).
5. Y.-T. Wu, J. S. Siegel. *Chem. Rev.* **106**, 4843 (2006).
6. V. M. Tsefrikas, L. T. Scott. *Chem. Rev.* **106**, 4868 (2006).
7. S. Higashibayashi, H. Sakurai. *Chem. Lett.* **40**, 122 (2011).
8. M. A. Petrukhina, L. T. Scott. *Fragments of Fullerenes and Carbon Nanotubes: Designed Synthesis, Unusual Reactions, and Coordination Chemistry*, John Wiley, New Jersey (2011).
9. T. Amaya, T. Hirao. *Chem. Commun.* **47**, 10524 (2011).
10. J. C. Hanson, C. E. Nordman. *Acta Crystallogr., Sect. B* **32**, 1147 (1976).
11. L. T. Scott, M. M. Hashemi, M. S. Bratcher. *J. Am. Chem. Soc.* **114**, 1920 (1992).
12. A. Sygula, A. H. Abdourazak, P. W. Rabideau. *J. Am. Chem. Soc.* **118**, 339 (1996).
13. Z. Marcinow, A. Sygula, A. Ellern, P. W. Rabideau. *Org. Lett.* **3**, 3527 (2001).
14. T. J. Seiders, K. K. Baldridge, G. H. Grube, J. S. Siegel. *J. Am. Chem. Soc.* **123**, 517 (2001).
15. H. Sakurai, T. Daiko, T. Hirao. *Science* **301**, 1878 (2003).
16. H. Sakurai, T. Daiko, H. Sakane, T. Amaya, T. Hirao. *J. Am. Chem. Soc.* **127**, 11580 (2005).
17. T. Amaya, K. Mori, H.-L. Wu, S. Ishida, J. Nakamura, K. Murata, T. Hirao. *Chem. Commun.* 1902 (2007).
18. T. Amaya, T. Nakata, T. Hirao. *J. Am. Chem. Soc.* **131**, 10810 (2009).
19. T. Amaya, M. Hifumi, M. Okada, Y. Shimizu, T. Moriuchi, K. Segawa, Y. Ando, T. Hirao. *J. Org. Chem.* **76**, 8049 (2011).
20. T. Amaya, H. Sakane, T. Muneishi, T. Hirao. *Chem. Commun.* 765 (2008).
21. T. Amaya, S. Seki, T. Moriuchi, K. Nakamoto, T. Nakata, H. Sakane, A. Saeki, S. Tagawa, T. Hirao. *J. Am. Chem. Soc.* **131**, 408 (2009).
22. M. A. Petrukhina, L. T. Scott. *Dalton Trans.* 2969 (2005).
23. M. A. Petrukhina. *Angew. Chem., Int. Ed.* **47**, 1550 (2008).
24. T. Amaya, H. Sakane, T. Hirao. *Angew. Chem., Int. Ed.* **46**, 8376 (2007).
25. H. Sakane, T. Amaya, T. Moriuchi, T. Hirao. *Angew. Chem., Int. Ed.* **48**, 1640 (2009).
26. P. Zanello, S. Fedi, F. F. de Biani, G. Giorgi, T. Amaya, H. Sakane, T. Hirao. *Dalton Trans.* 9192 (2009).
27. T. Amaya, W.-Z. Wang, H. Sakane, T. Moriuchi, T. Hirao. *Angew. Chem., Int. Ed.* **49**, 403 (2010).
28. S. Higashibayashi, H. Sakurai. *J. Am. Chem. Soc.* **130**, 8592 (2008).
29. R. Tsuruoka, S. Higashibayashi, T. Ishikawa, S. Toyota, H. Sakurai. *Chem. Lett.* **39**, 646 (2010).
30. U. D. Priyakumar, G. N. Sastry. *J. Phys. Chem. A* **105**, 4488 (2001).

31. T. Amaya, H. Sakane, T. Nakata, T. Hirao. *Pure Appl. Chem.* **82**, 969 (2010).